University of Groningen

Free energy of ionic hydration

Straatsma, T. P.; Berendsen, H. J. C.

Published in:
Journal of Chemical Physics

DOI:
10.1063/1.455539

IMPORTANT NOTE: You are advised to consult the publisher's version (publisher's PDF) if you wish to cite from it. Please check the document version below.

Document Version
Publisher's PDF, also known as Version of record

Publication date:
1988

Link to publication in University of Groningen/UMCG research database

Citation for published version (APA):
Straatsma, T. P., & Berendsen, H. J. C. (1988). Free energy of ionic hydration: Analysis of a thermodynamic integration technique to evaluate free energy differences by molecular dynamics simulations . *Journal of Chemical Physics*, *89*(9), 5876-5886. https://doi.org/10.1063/1.455539

Copyright
Other than for strictly personal use, it is not permitted to download or to forward/distribute the text or part of it without the consent of the author(s) and/or copyright holder(s), unless the work is under an open content license (like Creative Commons).

The publication may also be distributed here under the terms of Article 25fa of the Dutch Copyright Act, indicated by the “Taverne” license. More information can be found on the University of Groningen website: https://www.rug.nl/library/open-access/self-archiving-pure/taverne-amendment.

Take-down policy
If you believe that this document breaches copyright please contact us providing details, and we will remove access to the work immediately and investigate your claim.

Downloaded from the University of Groningen/UMCG research database (Pure): http://www.rug.nl/research/portal. For technical reasons the number of authors shown on this cover page is limited to 10 maximum.

Download date: 09-08-2022

Free energy of ionic hydration: Analysis of a thermodynamic integration technique to evaluate free energy differences by molecular dynamics simulations

T. P. Straatsma, and H. J. C. Berendsen

Citation: The Journal of Chemical Physics **89**, 5876 (1988); doi: 10.1063/1.455539
View online: https://doi.org/10.1063/1.455539
View Table of Contents: http://aip.scitation.org/toc/jcp/89/9
Published by the American Institute of Physics

Free energy of ionic hydration: Analysis of a thermodynamic integration technique to evaluate free energy differences by molecular dynamics simulations

T. P. Straatsma[a] and H. J. C. Berendsen[b]
*Laboratory of Physical Chemistry, University of Groningen, Nijenborgh 16, 9747AG Groningen,
The Netherlands*

(Received 18 January 1988; accepted 13 June 1988)

The thermodynamic integration technique to evaluate free energy differences by molecular dynamics simulations is analyzed. The hydration of the ions Na^+, K^+, Ca^{++}, F^-, Cl^-, and Br^- is used as the process to illustrate the potential utility of the method. A neon–water system is used as a reference system. The parameters that influence the performance and accuracy of the thermodynamic integration, in which the potential interaction parameters are gradually and continuously changed, are studied. These parameters include the total simulation time, the magnitude of the time step for the numerical integration of the equations of motion, the system size, and the cutoff radii for the intermolecular interactions. Fast convergence is found for the Gibbs free energy difference between Ne and Na^+ with respect to total simulation time. The time step and system size are relatively unimportant. The use of cutoff radii, for the ion–water but especially unfortunately also the water–water intermolecular interactions, seriously influences the results obtained. A simple correction for the use of cutoff radii cannot be made. Results are compared to experimental values.

I. INTRODUCTION

In a former article on the evaluation of free energy differences within the framework of molecular dynamics simulations, we reported an analysis of a statistical perturbation method using statistical reference ensembles and a thermodynamic integration technique. The process used to illustrate the methods was the hydrophobic hydration.[1] It was concluded that the perturbation method is practicable only for small free energy differences, less than about $2RT$. In this article we present a more detailed analysis of the thermodynamic integration technique to obtain free energy differences. In order to show the potential applicability of this method, even for large free energy differences, the hydration of monoatomic ions is used as an illustration.

The solvation properties of electrolytes in aqueous solution are of particular importance in solution chemistry. In many chemical and biochemical processes ionic hydration plays a very important role. One of the earliest models proposed for the free energy of ion hydration by Born[2] forms the basis for a continuum approach.[3] The free energy of hydration of ions is found from the reversible work required to charge a conducting hard sphere of radius r, embedded in a fluid at constant temperature and pressure, treated as a polarizable dielectric with relative dielectric constant ϵ_r,

$$\Delta G = -\frac{N_A z^2 e^2}{8\pi\epsilon_0 r}\left(1 - \frac{1}{\epsilon_r}\right). \qquad (1)$$

Here ze is the charge of the ion. In the Born approximation the free energy of ionic hydration depends on only two parameters, the ionic radius r and the relative dielectric constant ϵ_r of the fluid. Quantitatively the Born model is rather inaccurate, the deficiencies being the hard sphere assumption for the ionic solute, and the treatment of the solvent as a continuous dielectric. For positively and negatively charged ions with equal radii, the model predicts numerically equal free energies of hydration, although the structure of the water molecules around the ions will be quite different. Improved agreement with experimental values is obtained if the ionic radii are corrected with a correction term. The magnitude of this correction term only depends on the type of ion, anion or cation.[4] Another attempt to improve the model is a different treatment of the dielectric constant, being reduced in value for regions vicinal to the ions, due to dielectric saturation.[5] This approach has been refined by a number of authors.[6-8]

An attempt to incorporate solute intramolecular interactions and specific solute–solvent interactions for solvent molecules in the vicinity of the solute, while still using the continuum approach for the solvent at larger distances, has led to the development of a statistical thermodynamic supermolecule continuum model.[9,10] The model involves the evaluation of the partition function for the system containing the solute molecule and the solvent molecules of the first solvation shell, treating the bulk solvent effects by embedding this system in a polarizable dielectric continuum. The solute intramolecular and discrete solute–solvent interaction energies are evaluated from theoretical or semiempirical models for a large number of configurations. The interaction

---

[a] Present address: Chemistry Department, University of Houston, 4800 Calhoun Road, Houston, Texas 77004.

[b] Address for correspondence: Laboratory of Physical Chemistry, University of Groningen, Nijenborgh 16, 9747 AG Groningen, The Netherlands.

energy with the dielectric continuum is evaluated treating the supermolecule as an assembly of charges embedded in the dielectric. The contribution due to the presence of the dielectric continuum to the free energy of a configuration of charges is easily evaluated.[11,12] The free energy of a distribution of N point charges inside a cavity with radius a in a dielectric continuum with relative dielectric constant ϵ_r is given by

$$\Delta G = \frac{1}{8\pi\epsilon_0} \sum_{n=0}^{\infty} \frac{(n+1)(1-\epsilon_r)}{(n+1)\epsilon_r + n} \left(\frac{Q_n}{a^{2n+1}} \right), \tag{2}$$

where Q_n is the square of the nth moment of the charge distribution,

$$Q_n = e^2 \sum_{k=1}^{N} \sum_{l=1}^{N} z_k z_l r_k^n r_l^n P_n(\cos\theta_{kl}). \tag{3}$$

$P_n(\cos\theta_{kl})$ is a simple Legendre polynomial, $z_k e$ is the charge of the k th point charge, and r_k is its distance from the center of the cavity. For $n = 0$, $Q_0 = z^2 e^2$, where ze is the net charge of the distribution, leading to the Born charging energy. $Q_1 = \mu^2$, where μ is the total dipole moment of the distribution leading to the dipole polarization of the Onsager reaction field[13] contribution. The number of configurations that should be treated, a major problem in evaluating partition functions directly, can be reduced by a number of methods. In the shell methods the discrete solvent molecules are restricted to regions in space immediately vicinal to the solute. In the cell method each of the solvent molecules is restricted to a small region within the solvent shell. The site method is an extreme of the restriction of solvent molecules. Here the centers of mass of each solvent molecule are fixed to some low energy arrangement permitting the molecules only to have rotational degrees of freedom.

Electrostatic studies performed by Spears[14–16] and by Gowda and Benson,[17,18] computer simulation studies,[19] and quantum chemical Hartree–Fock studies[20] on monovalent ion water clusters yielded results in reasonable agreement with experimental values.[21,22] The calculated energies in these studies were systematically somewhat too low. Improved agreement with experiment was obtained by including three body interactions.[23–25]

In recent years a large number of computer simulation studies has been reported on dilute aqueous solutions of ions, giving insight into a variety of aspects of these solutions. The structure of water around a simple monovalent ion has been studied in terms of changed hydrogen bonding in vicinal water,[26] radial pair distribution functions,[27,28] and translational and rotational motion of the vicinal water molecules.[29-33] Comparisons of the solvation of a Na^+ ion in water and tetrahydrofuran,[34] and the hydration of the more complex ammonium and carboxylate ions[35] have been reported. Aqueous solutions of LiI in the vicinity of Lennard-Jones walls have been studied[36] and the reorientational motion of water in the vicinity of a neutral solute that is suddenly ionized has been investigated.[37] The list of citations is far from complete and illustrates the recently increased interest in these systems. All cited simulation studies were published within the last seven years.

II. THERMODYNAMIC INTEGRATION

The method of thermodynamic integration is a technique to calculate free energy differences that best corresponds to the general idea of how to measure the change in free energy of a system when some parameter specifying the thermodynamic state is slowly varied, and that is, therefore, now widely used. It is an accurate and straightforward method that does not suffer from the high density and large system problems encountered in most other methods.

In the usual thermodynamic integration the free energy difference is evaluated by performing a number of computer simulations along an isotherm to obtain values for p, or along an isochore to obtain values for U, that are then fitted to a polynomial.

The thermodynamic integration variables are not restricted to volume or temperature. If the intermolecular interaction is made, some function of a control variable λ, the Hamiltonian of the system, and thus the partition function Z, will be a function of λ as well. As a consequence the Helmholtz free energy also depends on λ,

$$F(\lambda) = -k_B T \ln Z(\lambda). \tag{4}$$

Differentiating $F(\lambda)$ with respect to λ then gives[38,39]

$$\frac{\partial F(\lambda)}{\partial \lambda} = -\frac{k_B T}{Z(\lambda)} \left(\frac{\partial Z(\lambda)}{\partial \lambda} \right) \tag{5}$$

$$= \int \frac{\partial \mathscr{H}(\lambda)}{\partial \lambda} \exp\left(-\frac{U(\lambda)}{k_B T} \right) d\mathbf{q}^N \Big/ \int \exp\left(-\frac{U(\lambda)}{k_B T} \right) d\mathbf{q}^N \tag{6}$$

$$= \left\langle \frac{\partial \mathscr{H}(\lambda)}{\partial \lambda} \right\rangle_\lambda \tag{7}$$

which is a canonical average of the mechanical quantity $\partial \mathscr{H}(\lambda)/\partial \lambda$ for a system with Hamiltonian $\mathscr{H}(\lambda)$. This average can simply be obtained from any computer simulation calculation.

The Helmholtz free energy difference between two states of a system with $\lambda = 0$ and $\lambda = 1$ can be found from integration of Eq. (7),

$$\Delta F = F(\lambda = 1) - F(\lambda = 0) = \int_0^1 \left\langle \frac{\partial \mathscr{H}(\lambda)}{\partial \lambda} \right\rangle_\lambda d\lambda. \tag{8}$$

As in the case for temperature or volume as the integration variables, computer simulations are performed for a number of λ values, ranging from 0 to 1. Fitting of the averages $\langle \partial \mathscr{H}(\lambda)/\partial \lambda \rangle_\lambda$, that can be evaluated very accurately if the simulations are sufficiently long, for each of these calculations permits the evaluation of the Helmholtz free energy difference by integration of the fitted function via Eq. (8).

A recent development is the thermodynamic integration to be carried out during the simulation itself.[1,40–42] Starting with an initial configuration obtained from an equilibrated ensemble representative for a system with Hamiltonian $\mathscr{H}_0 = \mathscr{H}(\lambda = 0)$ a molecular dynamics simulation is performed in which the parameter λ is smoothly changed from 0 to 1 with small increments $\Delta\lambda$ every dynamics step. If after N steps λ has reached the value 1, the free energy is found from Eq. (8), rewritten as a direct summation over the dynamics steps,

$$\Delta F = F(\lambda = 1) - F(\lambda = 0) = \sum_{i=1}^{N} \left\langle \frac{\partial \mathcal{H}(\lambda)}{\partial \lambda} \right\rangle_i (\Delta\lambda)_i$$

$$= \sum_{i=1}^{N} \Delta F_i, \tag{9}$$

where i counts the number of steps. In fact $\langle \partial \mathcal{H}(\lambda)/\partial \lambda \rangle_i$ no longer is an ensemble average, since it is evaluated from the configuration obtained in the ith step only. In order to obtain reliable results this configuration should be representative for a system with Hamiltonian $\mathcal{H}(\lambda_i)$. The change in λ, therefore, has to be so slow as to maintain the configurations essentially in equilibrium during the entire simulation. The change in λ then represents a reversible process, and the integration yields the work done during this process. The configuration of particles always lags behind the Hamiltonian, i.e., is representative for the Hamiltonian at an earlier time. Not permitting the configuration to equilibrate fully will result in computed values of ΔF that are too high. Since this is true for a simulation integrating from $\lambda = 1$ to $\lambda = 0$ as well, performing the thermodynamic integration back and forth leads to two values of ΔF, the difference whereof is a measure for the systematic error made. This hysteresis will decrease with increasing number of dynamics steps in which λ changes from 0 to 1. To minimize the systematic error the parameter λ should be changed every step such that ΔF varies as linearly as possible, i.e., the individual contributions ΔF_i should differ in magnitude as little as possible. This can be achieved by varying λ as some, in general nonlinear, function of time, or by choosing a different λ dependency of the Hamiltonian[43] such that initial and final Hamiltonians remain the same, but another path in the Hamiltonian space is taken as λ changes from 0 to 1. Unfortunately the best possible choice in general is not easy to guess beforehand.

Since no averaging over an ensemble of configurations is done, a statistical error cannot be examined.

Recently Mezei[44] proposed a finite difference thermodynamic integration method that combines a statistical perturbation method with the thermodynamic integration. For small intervals between initial and final states, derivatives of the Hamiltonian with respect to some scaling parameter λ are evaluated by the perturbation method. The obtained values $\Delta F(\lambda_i)/\Delta\lambda_i$ for the intervals i are then used to perform the thermodynamic integration. The perturbation results for intermediate simulations had earlier been used in a graphical determination of the free energy of cavity formation in water as a function of the cavity size.[42,45]

Simulations of isothermal–isobaric ensembles can be performed by techniques using modified Hamiltonians,[46,47] for which free energy difference methods have been proposed.[48] The thermodynamic integration technique was studied using molecular dynamics simulations of isothermal–isobaric ensembles, using the approach of weak coupling to an external bath. In the thermodynamic integration, the Hamiltonian is a function of some scaling parameter λ, $\mathcal{H} = \mathcal{H}(\lambda)$. The Gibbs free energy G, the fundamental thermodynamic property for isothermal isobaric ensembles, then is a function of λ as well,

$$G(\lambda) = -k_B T \ln \Delta(\lambda), \tag{10}$$

where $\Delta(\lambda)$ is the isothermal–isobaric partition function,[49]

$$\Delta(\lambda) = \frac{1}{h^{3N} N!} \int\int\int \exp\left(-\frac{\mathcal{H}(\lambda) + pV}{k_B T} \right) \times dV\, d\mathbf{p}^N d\mathbf{q}^N. \tag{11}$$

Differentiating $G(\lambda)$ with respect to λ then leads to

$$\frac{\partial G(\lambda)}{\partial \lambda} = \left\langle \frac{\partial \mathcal{H}(\lambda)}{\partial \lambda} \right\rangle_\lambda, \tag{12}$$

where the averaging is over the ensemble belonging to λ. The free energy difference between two systems for which λ is zero and unity then can be evaluated from integration of Eq. (12),

$$\Delta G = \int_0^1 \left\langle \frac{\partial \mathcal{H}(\lambda)}{\partial \lambda} \right\rangle_\lambda d\lambda. \tag{13}$$

The conditions and limitations that must be considered do not differ from the application of the methods to canonical ensembles.

III. COMPUTATIONAL DETAILS

A. Molecular dynamics simulations

The molecular dynamics simulations to study the thermodynamic integration technique applied to an ion in aqueous solution were performed using an isothermal–isobaric simulation algorithm. Weak coupling to an external temperature bath of 298 K with a coupling time constant of 0.4 ps, and to an external pressure bath of 1.0×10^5 Pa with a coupling time constant of 0.5 ps was used to maintain temperature and pressure in all simulations. The leap frog integration algorithm used included velocity and coordinate rescaling at every dynamics step to accomplish the weak coupling.[50]

Single atom ions were studied in systems consisting of the ion and 216 or 512 water molecules. The systems were treated in a cubic box, subjected to periodic boundary conditions. For the 216 water molecule system all intermolecular interactions were cutoff at 0.9 nm. Simulations of the 512 water molecules systems used a water intermolecular cutoff distance of 0.9 nm, while for the water–ion interactions different cutoff distances were used ranging from 0.9 to 1.2 nm.

In the reported simulations the intramolecular degrees of freedom of the water molecules were treated as separable constraints, using the SHAKE coordinate resetting procedure.[51–53] Except for one simulation the time step used was 0.001 ps.

B. Intermolecular potentials

The model potential for the water intermolecular interactions used in the molecular dynamics simulations reported here, is the simple point charge (SPC) model developed by Berendsen *et al.*[42] and Postma.[54] The geometry of the water molecule is identical to the well known ST2 model of Stillinger and Rahman,[55] with an oxygen–hydrogen distance r_{OH} of 0.1 nm and a tetrahedral bond angle of 109.47°. The charge distribution is similar to the three point charge central force model,[56] with the point charges situated on the nuclei. This arrangement allows a simple description of the permanent dipole and the directional dependency of the electrostatic interactions. On the oxygen nucleus an additional 6–12 Lennard-Jones potential is situated. The full potential between a pair of water molecules can thus be written as

$$\Phi = -\left(\frac{A}{r_{OO}}\right)^6 + \left(\frac{B}{r_{OO}}\right)^{12} + \frac{e^2}{4\pi\epsilon_0} \sum_{i=\mathrm{O,H,H}} \sum_{j=\mathrm{O,H,H}} \frac{z_i z_j}{r_{ij}}, \tag{14}$$

where i and j sum over the nuclei of one water molecule. The parameter A, accounting for the dispersion energy was obtained from experiment,[57] $A = 0.317\,22$ nm$(\mathrm{kJ\cdot mol^{-1}})^{1/6}$. The repulsion parameter B and the charges z_H on the hydrogen sites and $z_O = -2z_H$ on the oxygen nuclei were optimized with the use of molecular dynamics simulations as to yield the correct value for the potential energy when used for a system of water molecules representing the liquid state, and to obtain the experimental liquid densities in simulations at normal pressure. The radial oxygen–oxygen distribution function obtained from a molecular dynamics simulation should be qualitatively comparable to experimental findings. From a series of simulations using a range of values for B and $z_O = -2z_H$, the best parameters that fulfill the imposed criteria were found to be $B = 0.3428$ nm$(\mathrm{kJ\cdot mol^{-1}})^{1/12}$ and $z_O = -2z_H = -0.82$. Considering the simplicity of the model the results that can be obtained are satisfactory for liquid water,[42] the hydration of proteins,[58] and small organic compounds.[59] Comparison of the model with other water models was reported by Beveridge *et al.*[60] and Jorgensen.[61]

Much attention has been given to the calculation of intermolecular monovalent ion water energy surfaces from quantum chemical computations. Especially the extensive Hartree–Fock SCF studies of the energy surface of one water molecule in the field of the simple monoatomic ions in a large number of different configurations reported by Clementi and Popkie[62] and Kistenmacher *et al.*[63–65] have been frequently used to obtain analytic functions for the water ion interaction potentials. A very extensive study on the SCF potential energy surface for $\mathrm{Na^+}$ and $\mathrm{Cl^-}$ ions interacting with one water molecule in a very large number of configurations was reported by Dacre[66] recently. A special method to obtain ion–water potential functions using SCF gradient calculations was given by Bounds and Bounds.[67,68] Results of SCF calculations using pseudopotentials were reported for the divalent ions $\mathrm{Mg^{++}}$ and $\mathrm{Ca^{++}}$ by Ortega.[69] *Ab initio* results were also obtained for clusters of one to six water molecules and one monovalent ion.[70–72]

The ion–water interaction potentials used in this study are described by a Coulombic interaction of the ion with the oxygen and hydrogen point charges of the SPC water model, which are left unchanged. In addition, there is a Lennard-Jones 6–12 potential acting between the ion and the SPC oxygen atoms. In order to keep a physically realistic picture of the system, the ion charges were given their natural values. The Lennard-Jones parameters for the ions were obtained as follows. For the $\mathrm{Na^+}$ and $\mathrm{K^+}$ ions these parameters resulted from a weighted least squares fit of the energies of a number of SPC water–ion arrangements to the HF-SCF energies obtained by Kistenmacher *et al.*[63] for the water-molecule–ion pair. The weighting ensured the best fit for the lowest energy regions thereby yielding an optimal ion size, and is based on the assumption that these low energy conformations will be the most frequent and important ones in the solution system as well. A similar least squares fit to HF-SCF energies obtained by Dacre,[66] resulted in similar parameters for $\mathrm{Na^+}$. For $\mathrm{F^-}$ parameters were obtained in much the same way using the HF-SCF results reported by Kistenmacher *et al.*[64] Lennard-Jones parameters used for the ions $\mathrm{Cl^-}$ and $\mathrm{Br^-}$ were those reported by van Gunsteren,[73] and the parameters for $\mathrm{Ca^{++}}$ were taken to be those used by Teleman.[74,75] The parameters are collected in Table I.

Since the parameters are fitted to HF-SCF energies obtained for the water-molecule–ion pair, dispersion effects are not taken into account. The polarization of the ion is relatively unimportant, whereas the polarization of the water molecules by the ion is believed to be a considerable effect, responsible for about 20% of the internal energy.[76] At least part of this polarization energy contribution is included through the enhanced SPC charges.

IV. EQUILIBRIUM PROPERTIES

Some properties obtained from the equilibration simulations of the ion–water systems are given in Table II. The shape and positions of the peaks in the radial pair distribution functions for the sodium cation–water ensemble, as well as the coordination number of the first shell, are in good agreement with results reported for other simulation studies.[27,31,32] The energetic contributions to the ionic solvation given in Table II are in reasonable accordance with previously reported results.[27]

For the potassium cation–water ensemble the position and shape of the peaks in the radial pair distribution functions are in accordance with results obtained by Mezei and Beveridge[27] and Nguyen and Adelman.[31] The same coordination for the first hydration shell is also found. The second peaks in the distribution functions found by these authors are significantly more pronounced however. In addition, the energetic contribution to the solvation given in Table II,

TABLE I. SPC water–ion interaction potential parameters.

Ion	ϵ/k_B (K)	σ (nm)	z_s
$\mathrm{Na^+}$	24.12	0.285	1
$\mathrm{K^+}$	0.73	0.452	1
$\mathrm{Ca^{++}}$	76.73	0.317	2
$\mathrm{F^-}$	66.61	0.305	-1
$\mathrm{Cl^-}$	64.69	0.375	-1
$\mathrm{Br^-}$	59.47	0.383	-1

TABLE II. Equilibrium results for the ion–water systems. Values in parentheses give the statistical errors.

	Na^+	K^+	Ca^{++}
n_{H_2O}	512	216	512
R_c/nm	0.9	0.9	1.2
Time/ps	15	10	10
Temperature/K	312.3(0.4)	317.0(1.0)	319.3(0.5)
Pressure/10^5 Pa	− 4(25)	− 6(42)	− 1(31)
Volume/nm^3	15.93(0.02)	6.88(0.02)	16.58(0.02)
U^{pot}_{ws}/kJ mol^{-1}	− 799(5)	− 559(5)	− 2 628(6)
U^{kin}_{s}/kJ mol^{-1}	3.7(0.2)	4.3(0.4)	4.3(0.2)
U^{tot}_{ws}/kJ mol^{-1}	− 795(5)	− 554(5)	− 2 623(6)
U^{pot}/kJ mol^{-1}	− 21 462(11)	− 9063(8)	− 22 081(14)
U^{kin}/kJ mol^{-1}	3 996(5)	1716(5)	4 082(7)
U^{tot}/kJ mol^{-1}	− 17 466(12)	− 7347(8)	− 17 999(14)
n_{H_2O} (1st shell)	5.5	7	9.0
	F^-	Cl^-	Br^-
n_{H_2O}	216	216	216
R_c/nm	0.9	0.9	0.9
Time/ps	10	20	20
Temperature/K	315.9(0.7)	317.0(0.5)	316.9(0.5)
Pressure/10^5 Pa	42(45)	− 2(34)	− 9(27)
Volume/nm^3	7.46(0.03)	7.11(0.01)	7.10(0.01)
U^{pot}_{ws}/kJ mol^{-1}	− 823(5)	− 532(3)	− 521(3)
U^{kin}_{s}/kJ mol^{-1}	4.2(0.2)	4.3(0.2)	3.7(0.2)
U^{tot}_{ws}/kJ mol^{-1}	− 819(5)	− 528(4)	− 518(3)
U^{pot}/kJ mol^{-1}	− 9 040(11)	− 8969(9)	− 8 956 (4)
U^{kin}/kJ mol^{-1}	11 711(4)	1715(3)	1 717(3)
U^{tot}/kJ mol^{-1}	− 7 329(14)	− 7254(9)	− 7 240(4)
n_{H_2O} (1st shell)	6.0	7	7

− 559 kJ mol^{-1}, is considerably more negative than the value of − 460 kJ mol^{-1} that was reported by Mezei and Beveridge,[27] in which the MCY potential[77] was used for the water intermolecular interactions and water–ion potentials were fitted to the *ab initio* results of Kistenmacher *et al.*[63]

The same discrepancy in the energetic contribution of the ion solvation was found for the fluoride anion–water ensemble. The radial pair distribution functions are in very good agreement, however, showing the same characteristic pattern at the same radial distances. Also the coordination number for the first hydration shell is in good agreement. This coordination number can be evaluated easily in this case, since the radial pair distribution function drops to zero after the first peak.

The shape of the chloride anion–water distribution functions and the running coordinate numbers are in good agreement with earlier reported results.[27,28] The energetic contribution to the solvation is in accordance as well.

The general shape of the radial distribution functions for the bromide ion is very similar to the corresponding functions for chloride. The peaks are only slightly shifted outward, and the second peak in the oxygen–ion distribution function is somewhat more pronounced. In both cases the coordination in the first shell is about seven. The energetic contributions U^{pot}_{ws} for these ions also are very similar.

V. RESULTS

A. Total simulation time

One of the aspects determining the accuracy of the thermodynamic integration technique to obtain free energy differences is the rate at which the Hamiltonian is changed during the simulation. To determine the influence of the number of time steps taken in a thermodynamic integration simulation on the accuracy of the evaluated free energy difference, a number of molecular dynamics simulations were performed in which a hydrated neon atom is linearly changed into a sodium cation. This change represents a drastic change in the system, since a long ranging Coulombic interaction is introduced. Five simulations were performed for this process with total simulation times of 5, 10, 20, 40, and 80 ps. All other parameters were kept the same. The simulation box contained 216 water molecules. The ion–water and water–water interactions were cut off at radial distances of 0.9 nm. The time step in all simulations was 0.001 ps. In five additional simulations the reverse process was performed, changing the sodium cation back into a neon atom, under conditions identical to the forward processes. The forward runs were started from a neon–water configuration obtained after an equilibration of the system for 50 ps. The configuration with which the reverse simulations were started was obtained from a 5 ps equilibration simulation of the sodium cation–water system.

The free energy differences obtained for the simulations are summarized in Table III. In this table the results for the forward processes are labeled $\Delta G_i^{\rightarrow}$, while the reverse free energy differences are denoted $\Delta G_i^{\leftarrow}$. For the forward and reverse simulations, changing neon into a sodium cation and vice versa, the Gibbs free energy is depicted as a function of the simulation time in Fig. 1. The first noteworthy feature is the smoothness of both curves, showing hardly any fluctuations. This behavior is found for all thermodynamic integration simulations for which results are given in Table III. In cases where $\Delta G_i^{\rightarrow}$ and $\Delta G_i^{\leftarrow}$ are considerably different for forward and reverse simulation of the same process, the hysteresis can therefore not be explained from fluctuations in the free energy curves. The hysteresis has to be explained from the inability of the configurations to follow the changing Hamiltonian. The second observation from Fig. 1 is that the free energy changes for the forward and reverse simulations practically coincide, leading to a very small hysteresis of 1.44 kJ mol^{-1}. This is also found in the simulation for the same process in which the Hamiltonian was changed in 40 ps. There the hysteresis is even somewhat smaller, 0.30 kJ mol^{-1}. Decreasing the total simulation time further leads to a rapid increase of the hysteresis. In the simulations in 5, 10, and 20 ps obviously the changes in the Hamiltonian are made too rapidly and the configurations cannot be considered representative for the Hamiltonian used at that time step at which they are generated. Considering the important reorientation of the water molecules in the vicinity of the solute obtaining a charge in the process, the accuracy of the thermodynamic integration in only 40 ps is surprisingly good.

In Fig. 2 the free energy differences of the neon to sodium cation thermodynamic integrations are shown graphically, as a function of the total simulation time. Note that the free energy differences are all given with respect to the neon–water system. The simulation results discussed thus far are indicated with ○ in this picture. Both forward and reverse simulations rapidly approach the value of approximately -421 kJ mol^{-1} for the free energy difference between neon and sodium cation hydration. The average values for the ΔG_i's obtained from the forward and reverse simulations, even for cases with large hysteresis, are in good agreement with this value. The results obtained here give insufficient information, however, to conclude that this will be true in general.

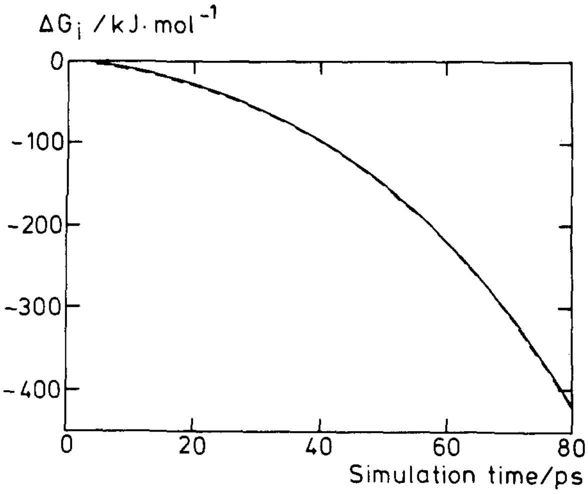

FIG. 1. Free energy of hydration change in a thermodynamic integration from neon to a sodium cation in 80 ps. The dashed curve gives the free energy change of the reverse process.

B. Time step

A time step of 0.002 ps still gives stable simulations, but with increased inaccuracy. The influence of the time step can be seen in Table III, where the results given for a thermodynamic integration from neon to a sodium cation in 40 ps, using twice as large a time step, 0.002 ps. Compared to the 40 ps simulations using 0.001 ps time steps, results get worse. The hysteresis is considerably larger. This indicates that the inaccuracy introduced by the larger time step is not without consequence for the evaluation of free energies. Compared to the 20 ps simulation using 0.001 ps time steps, involving an equal number of dynamics steps, the results are improved. Both forward and reverse simulations result in values for $\Delta G_i^{\rightarrow}$ and $\Delta G_i^{\leftarrow}$ closer to those obtained from the more accu-

TABLE III. Free energy of hydration differences between a neon atom and a sodim cation by thermodynamic integration for a number of parameter settings.

T		R_{ww}	R_{ws}	Δt	$\Delta G_i^{\rightarrow}$	$\Delta G_i^{\leftarrow}$	Hyst.
(ps)	n_W	(nm)		(ps)	(kJ mol^{-1})		
5	216	0.9	0.9	0.001	− 401.90	441.20	39.30
10	216	0.9	0.9	0.001	− 404.38	432.93	28.55
20	216	0.9	0.9	0.001	− 411.07	429.37	18.30
40	216	0.9	0.9	0.001	− 420.66	420.96	0.30
80	216	0.9	0.9	0.001	− 420.75	422.19	1.44
40	216	0.9	0.9	0.002	− 416.05	424.76	8.71
40	512	0.9	0.9	0.001	− 423.90		
40	512	0.9	1.05	0.001	− 443.63		
40	512	0.9	1.2	0.001	− 460.63		
40	512	1.2	0.9	0.001	− 403.84		
40	512	1.2	1.2	0.001	− 429.07		

rate long time simulations. Consequently the hysteresis is smaller, 8.71 kJ mol^{-1}, compared to the value 18.30 kJ mol^{-1} for the 20 ps simulation using 0.001 ps time steps. The ΔG_i are indicated with □ in Fig. 2.

C. System size

Results discussed in the previous sections were obtained from simulations of a system containing 216 water molecules. The cutoff radius used was only slightly less than half the box size. None of the water molecules therefore is influenced directly by the presence of periodic images of the central ion in the neighboring boxes. However, water molecules within the interaction radius of the central ion will be influenced indirectly by neighboring ion images through other water molecules in those neighboring boxes. Since all ion images have like charges, this will result in an increase of the absolute free energy of the system, as compared to a system with an ion in infinite dilution. The effect is in principle also present in simulations of a neutral solute in water. The interaction range of a neutral solute is much smaller, however, than for an ionic solute. For neutral solutes the effect on the free energy of hydration will therefore be much smaller. Given the fact that this effect becomes important when the solute is slowly charged, a contribution to the free energy difference between the neutral and ionic solute, as calculated with the thermodynamic integration technique, is to be expected due to this effect.

To obtain an impression on the importance of this effect, a 40 ps thermodynamic integration simulation was performed for neon to a sodium cation in a periodic box containing 512 instead of 216 water molecules. The ion–water cutoff radius was kept the same, 0.9 nm. Compared to the simulation with 216 water molecules the Gibbs free energy difference is indeed lowered. The amount, -3.36 kJ mol^{-1}, is small compared to the total free energy difference however. Apparently at cutoff radii of 0.9 nm this effect is of minor importance. The free energy difference obtained with respect to the neon–water ensemble is indicated with ◇ in Fig. 2.

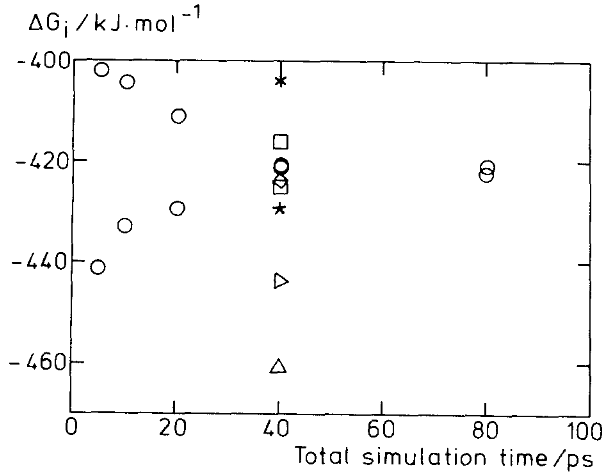

FIG. 2. Free energy of hydration difference between neon and a sodium cation as a function of total simulation time from thermodynamic integration results. The number of water molecules in the simulation box, the water intermolecular cutoff, the solute–water intermolecular cutoff and the time step are, respectively, for ○: 216, 0.9 nm, 0.9 nm, and 0.001 ps, for □: 216, 0.9 nm, 0.9 nm, and 0.002 ps, for ◇: 512, 0.9 nm, 0.9 nm, and 0.001 ps, for ▷: 512, 0.9 nm, 1.05 nm, and 0.001 ps, for △: 512, 0.9 nm, 1.2 nm, and 0.001 ps, for ⋆: 512, 1.2 nm, 1.2 nm, and 0.001 ps, and for *: 512, 1.2 nm, 0.9 nm, and 0.001 ps.

D. Cutoff radii

For long range interactions, as the Coulombic interactions, the use of cutoff radii is expected to have serious consequences.[78] In the simulations the interactions were truncated at 0.9 nm. As a simple and easily evaluated approximation of a correction to the difference in free energy of hydration between a neutral solute and an ion, Born's approximation, Eq. (1), can be used. With the assumption that the solvent beyond 0.9 nm from the ion may be treated as a dielectric continuum with dielectric constant $\epsilon_r = 80$, this correction to the free energy of hydration becomes for a monovalent ion -76.22 kJ mol^{-1}. This value is rather large compared to the free energy difference with the neon–water ensemble. Unfortunately, this correction decreases only slowly with increasing cutoff radius, since from Born's equation the Gibbs free energy of a charge distribution in a cavity embedded in a dielectric is proportional to its reciprocal cavity radius.

To determine if the Born equation gives a sufficiently accurate approximation of the correction for the free energy of hydration of ions when cutoff radii are used, additional thermodynamic integrations were performed in which a neon atom as a solute in water was linearly changed into a sodium cation. The system contained 512 water molecules and used a 0.9 nm cutoff radius for the water intermolecular interactions and a truncation at 1.05 and 1.2 nm for the ion–water intermolecular potential interactions. The total simulations were performed in 40 ps, using time steps of 0.001 ps. The free energy of hydration ΔG_i, with respect to the neon–water system, is in Fig. 2 for the 1.05 nm solute–water cutoff radius indicated with ▷, for the 1.2 nm solute–water cutoff radius with △, and are found to be -443.63 and -460.63 kJ mol^{-1}, respectively. Compared to the thermodynamic integration, using an ion–water cutoff radius of 0.9 nm, but with all other parameters kept the same, the simulation with a solute–water cutoff radius of 1.2 nm shows a drop in Gibbs free energy of -36.73 kJ mol^{-1}. This is about twice the amount that would have been predicted from the Born equation, which is -19.05 kJ mol^{-1}. Other effects must be important therefore, leading to additional contributions to the free energy.

One possible effect is due to higher multipoles existing within the sphere around the central ion. These multipoles of the charge distribution made up by the ion and the surrounding water molecules embedded in the dielectric, give additional negative contributions to the free energy of hydration. Although the higher moments do not exist on the average, due to the symmetry of the system, they are present in the individual configurations. The effect is thus due to fluctuations of the system. It does not average to zero since the energy is quadratic in the multipole moments. The contributions were evaluated for the water molecules within a radius of 0.4 nm from a central negative ion, using a cavity radius of

0.9 nm. The radius of 0.4 nm ensures that all water molecules in the first shell are considered. Use of this value also prevents the inclusion of charges near the wall of the cavity, causing expression (2) to diverge. With this radius the contributions were found to converge rapidly and to be very small compared to the monopole contribution. Fluctuating higher multipoles therefore do not significantly contribute to the large drop in free energy if the cutoff radius is lengthened from 0.9 to 1.2 nm.

The cutoff radius used for the water intermolecular interactions may also influence the free energy of hydration of the ion as evaluated from the thermodynamic integration method. A central ion tends to polarize the surrounding water molecules in the radial direction, thus introducing a long range order that will affect the average water intermolecular interaction beyond their cutoff radius. Enlarged water intermolecular interaction cutoff radii may therefore also affect the orientation of water molecules in the field of the ion, leading to changes in the free energy of hydration of the ion. The importance of this effect was studied by performing simulations using a cutoff radius of the water intermolecular interactions of 1.2 nm instead of 0.9 nm, and cutoff radii for the solute–water interactions of 0.9 and 1.2 nm. The free energy differences between neon and the sodium cation in these cases are -403.84 and -429.07 kJ mol^{-1}. These values are indicated by ⋆ and * in Fig. 2. Compared to the simulations with a water intermolecular interaction cutoff of 0.9 nm, enlarging the solute–water cutoff radius leads to a smaller difference in free energy, -25.23 kJ mol^{-1} instead of -36.73 kJ mol^{-1}. This value is closer to the correction predicted using Born's equation, -19.05 kJ mol^{-1}. It is concluded, therefore, that the choice of the water intermolecular interaction cutoff is very important when evaluating free energy differences in these types of systems, especially when ionic species are involved. A value of 1.2 nm may still be somewhat too small for the system studied here.

From the simulations performed for the sodium cation–water system it is concluded that the truncation of Coulombic potentials considerably affects the results obtained from thermodynamic integration simulations if a charge is introduced into or removed from a system. The correction as evaluated from Born's equation is important, but inaccurate when relatively short cutoff radii are used. For thermodynamic integrations in which charges are present, but left unchanged, the corrections to the free energy needed may be similar in initial and final states, in which case the corrections cancel in the free energy difference of the two states. For cases in which charges are changed, however, a more satisfactory method for correction must be developed.

E. Comparison with experimental values

In Table IV a number of free energy differences are given that involve the ions Na^+, K^+, Ca^{++}, F^-, Cl^-, and Br^-. All results were obtained using the thermodynamic integration technique with linear changes of the Hamiltonian with respect to time. The free energy change as a function of time is a smooth curve in all cases. For those cases in which a reverse thermodynamic integration was performed the hysteresis found is small compared to the total free energy change. If the absolute values of the free energy of hydration for the initial solutes are known, the free energy of hydration of the ions can be evaluated from the results given in Table IV. The free energies of hydration obtained for the ions are given in Table V. The experimental values given are those published by Friedman and Krishan,[79] but corrected in order to give the free energy of transfer of an ion from its ideal gas phase to solution, both at standard concentration. This correction amounts to -7.92 kJ mol^{-1}, applied to the experimental values which represent the transfer of an ion from its ideal gas phase at standard pressure to ideal solution at 1 molar concentration. The corrections of the calculated values, mentioned in Tables IV and V, are the simple Born charging energies.

Using the value 10.36 kJ mol^{-1} for the Gibbs free energy of hydration of neon, the free energies of hydration of Na^+, K^+, and F^- can be obtained directly from one simulation. For Na^+, using the 216 and 512 water molecules systems, the free energy of hydration, including the Born correction, is -507.6 and -496.6 kJ mol^{-1}, respectively. The deviation from the experimental value, which is -419.2 kJ mol^{-1}, is about 20%. For the free energy of hydration of K^+, about the same deviation from the experimental result is found. The Born corrected value for K^+ is -424.8 kJ mol^{-1}, compared to an experimental value of -346.0 kJ mol^{-1}. For both Na^+ and K^+ the evaluated free energy of hydration is considerably too negative. Good

TABLE IV. Free energy differences obtained for a number of ions by themodynamic integration.

Process	T (ps)	$\Delta G^{\rightarrow}$ (kJ mol^{-1})	$\Delta G^{\leftarrow}$ (kJ mol^{-1})	Hyst. (kJ mol^{-1})	n_W	R_c (nm)	$\Delta G_i^{\mathrm{exp}}$ (kJ mol^{-1})
$Ne \rightarrow Na^+$	80	-420.75	422.19	1.44	216	0.9	-429.6
$Ne \rightarrow Na^+$	40	-429.07			512	1.2	-429.6
$Ne \rightarrow K^+$	80	-295.33	294.07	-1.26	216	0.9	-356.4
$Ne \rightarrow Ca^{++}$	80	-1383.45			512	1.2	-1611.6
$Ne \rightarrow F^-$	80	-410.48	410.23	-0.15	216	0.9	-452.6
$Na^+ \rightarrow K^+$	40	124.48	-123.11	1.37	216	0.9	73.2
$F^- \rightarrow Cl^-$	20	185.96	-177.27	8.69	216	0.9	117.2
$Cl^- \rightarrow Br^-$	20	11.01	-11.12	-0.11	216	0.9	13.8

TABLE V. Free energy of hydration of Na^+, K^+, Ca^{++}, F^-, Cl^-, and Br^-. Corrected values include the Born charging energy.

Ion	n_W	R_{ww}	R_{ws}	ΔG^0	ΔG^0_{corr}	ΔG^0_{exp}
				(kJ mol^{-1})		
Na^+	216	0.9	0.9	− 431.4	− 507.6	− 419.2
Na^+	512	1.2	1.2	− 439.4	− 496.6	− 419.2
K^+	216	0.9	0.9	− 348.6	− 424.8	− 346.0
Ca^{++}	512	0.9	1.2	− 1393.8	− 1622.5	− 1601.2
F^-	216	0.9	0.9	− 420.8	− 497.1	− 442.2
Cl^-	216	0.9	0.9	− 239.2	− 315.4	− 325.1
Br^-	216	0.9	0.9	− 228.2	− 304.4	− 311.3

agreement with experiment is found for the divalent ion Ca^{++}. The Born corrected theoretical value of − 1622.5 kJ mol^{-1} is relatively close to the experimental value of − 1601.2 kJ mol^{-1}.

The free energy change obtained from a thermodynamic integration in which Na^+ is linearly changed into K^+, is 123.4 kJ mol^{-1}. This value is consistent with the free energy difference as obtained from the thermodynamic integration results in which both ions are generated starting from a neon–water ensemble. The poor agreement of the calculated free energies of hydration of these ions with experimental results is most likely to be caused by ill-chosen potential parameters.

The calculated free energy of hydration of F^- is − 497.1 kJ mol^{-1}, which is again too negative compared to the experimental value. Changing the F^- anion in successive thermodynamic integrations into Cl^- and Br^-, also gives the free energy of hydration of these ions, which is − 315.4 and − 304.4 kJ mol^{-1}, respectively. These values are in good agreement with the experimental values − 325.1 and − 311.3 kJ mol^{-1}. The somewhat larger hysteresis in the thermodynamic integration of F^- into Cl^- is due to the short total simulation time, 20 ps, in which the change in the Hamiltonian was made.

Although the hysteresis is not expected to have negative values, in a few simulations it has. The absolute value however is in these cases very small compared to the total change in free energy. A negative hysteresis can in principle be found if the initial configuration for the thermodynamic integration is taken from a not fully equilibrated system. But even if taken from a well equilibrated system free energy changes may still be dependent on the particular configuration chosen to start the thermodynamic integration.

The computed free energy difference between the hydration of Cl^- and Br^- is only − 11.0 kJ mol^{-1} and can therefore also be obtained by employing the perturbation method. Treating the Br^- potential as a perturbation to a 20 ps molecular dynamics reference ensemble of Cl^- in 216 water molecules, yields a free energy difference of 11.0 ± 0.1 kJ mol^{-1}. With the Cl^- potential used as a perturbation to a 20 ps molecular dynamics ensemble of Br^- in 216 water molecules, a free energy difference of − 11.1 ± 0.1 kJ mol^{-1} is obtained. These values are in good agreement with the thermodynamic integration results, although the absolute values are well above the $2RT$ limit for the perturbative treatment in one step. A similar perturbation study was reported by Lybrand *et al.*[80] These authors used the same potential parameters for the Cl^-–water interaction potential, but modified the Br^-–water potential parameters in order to reproduce the experimental relative interaction energies. The free energy difference reported is very close to the experimental value. This is not surprising however since the potential energy difference (ΔU) is a first order approximation to the free energy difference (ΔG). Adjusting the potential parameters to obtain the experimental energy difference (ΔU) consequently leads to better results for (ΔG). The same reasoning is true for the results reported by Brooks[81] for a perturbation method analysis of the hydration of Cl^- and Br^- in which the same ion–water potentials were used.

F. Temperature drift

The thermodynamic integrations in which a charge is introduced into the system show a gradual increase of the temperature by about 6 K. This introduction of heat into the system is due to the use of cutoff radii. Since the entropy difference is small this negligibly influences the free energy difference.

VI. DISCUSSION

The free energy of hydration of the simple ions studied provide a good test for the thermodynamic integration method. The introduction of a charge in the system gives rise to drastic changes in the system and large free energy differences. It is surprising that converging results for the free energy difference between a hydrated neon atom and a sodium cation can be obtained already in only 40 000 dynamics steps. In all simulations in which the neutral solute atom was linearly changed into an ion, the free energy change as a function of simulation time was nonlinear, but monotonous. Improved accuracy of the results would therefore have been obtained if the time dependency of the integration variable λ was taken as a nonlinear function of time. Integrating from the neutral solute to the ion, the changes in λ could have been somewhat larger in the beginning and decreasing as the process proceeds. In these simulations results would have been more accurate also, if the time step was increased, keeping the total number of time steps the same.

One important aspect in the simulation studies of ionic solutions is the correction that is necessary when interaction potentials are truncated at some cutoff radius. From the two thermodynamic integrations in which neon is changed into a sodium cation, using different cutoff radii for the ion–water interactions, it can be seen that the influence is considerable. For the free energy of a system containing a net charge the Born charging energy represents an important but incomplete contribution to such a correction. The attempts made to account for the truncation effects[81] remain highly unsatisfactory.

The thermodynamic integration technique appears to be extremely sensitive to the model potentials chosen to describe the intermolecular interactions. The agreement with experimental free energies of hydration for the ions is rather poor in a number of cases. This emphasizes once more the importance of the availability of suitable intermolecular interaction potentials to represent real atoms and molecules. Another conclusion from the present study is that the fitting of potential parameters to *ab initio* calculations of solute–water molecule pairs will not always give satisfactory parameters that can be used for simulations of aqueous solutions. On the other hand, the thermodynamic integration method provides a sensible tool for the judgment of the validity of intermolecular potential parameters.

VII. CONCLUSION

From the results reported here the thermodynamic integration method appears to be a reliable and generally applicable technique to evaluate free energy differences. If the method is to be used, a number of decisions has to be made that may influence the accuracy of the results considerably. Principally the thermodynamic integration is used to evaluate the free energy difference between two systems by calculating the work required to make the reversible change from one system into the other. The method actually carries out the reversible process by changing the Hamiltonian at every dynamics step. To ensure reversibility the process must be carried out very smoothly. This is accomplished by requiring that the change in the Hamiltonian made every step is as small as possible. Reversibility can only be approached if the configuration generated at a particular step is representative for the Hamiltonian at that step. Strictly speaking, this can only be achieved if the changes in the Hamiltonian per time step are infinitely small. The measure to which this situation is approximated in practical simulations depends on the following considerations.

(i) *Total simulation time.* The change in the Hamiltonian that is made every time step can obviously be made smaller by increasing the number of time steps in which the total change in the Hamiltonian is made.

(ii) *Path of the Hamiltonian.* The free energy is a state function. As a consequence the free energy difference between two systems does not depend on the path followed when changing the Hamiltonian. With a judicious choice of the functional form of the integration variable dependency of the Hamiltonian, this path may be chosen such that the change per time step is as small as possible. The change in the Hamiltonian then leads to a free energy change per time step that is about equal in magnitude for all steps taken in the integration. The free energy change then has a linear dependency of time.

(iii) *Time dependency of the integration variable.* If the free energy change is monotonous as a function of time and the free energy change per time step is consistently increasing or consistently decreasing as the simulation proceeds, the results may be improved by making the integration variable λ some nonlinear function of the simulation time. This procedure may bring about the total free energy difference to be distributed over the total number of time steps as equable as possible. This does not change the path followed by the Hamiltonian however. If the system crosses a free energy barrier during the thermodynamic integration, results can only be improved by changing the integration variable dependency of the Hamiltonian.

(iv) *Time step.* In some cases, especially if translational or reorientational motions of particles will result from the changes in the Hamiltonian, increasing the time step for the numerical integration of the equations of motion will give the system more time to adapt to the changing Hamiltonian. If the number of time steps is kept the same, more accurate results for the free energy difference may then be found with the same computational effort. The numerical integration of the equations of motion will become less accurate however.

It is not always obvious how to determine the most appropriate settings of these parameters at forehand. It is therefore crucial, and fortunately easy, to monitor the free energy change as the thermodynamic integration simulation proceeds. In many cases it may be only afterwards that the parameter settings can be justified.

The best measure of the accuracy of the values obtained for the free energy differences is the hysteresis that may be obtained if the reverse process is studied by performing a thermodynamic integration under the same conditions. The hysteresis gives an indication of the systematic error caused by the time lag between the Hamiltonian and the actual configuration at every step. If only one simulation is performed, the accuracy may possibly be estimated from the behavior of the free energy change as a function of the simulation time and the largest free energy change that was made in a single dynamics step. This may give a rough estimate of the accuracy, but will be a matter of experience. From the present study the following guideline, to be interpreted with caution, may be given to obtain reasonable accurate results. If the free energy change in the simulation can be made approximately linear, the number of dynamics steps in which a free energy difference of 1 kJ mol^{-1} is made should at least be 100. For nonlinear behavior of this free energy change a general guideline cannot be given. Since the free energy change during the simulation can in principle have any shape, the statistical error is difficult to obtain.

Finally a remark should be made concerning the use of cutoff radii. Especially if long ranged interactions are involved in the change of the Hamiltonian, cutoff radii should be chosen with care. Unfortunately there is no method to systematically analyze the influence of the use of cutoff radii. Development of such a method should be considered, since simulations using cutoff radii so large that corrections to the free energy difference will be negligible will be extremely computer time consuming. All in all, the thermodynamic integration method may prove to be a sensible tool for the calculation of free energy differences. The method is more generally applicable than the majority of other methods suggested.

ACKNOWLEDGMENT

This work was supported in part by the Foundation for Chemical Research in the Netherlands (S.O.N.) under the auspices of the Netherlands Organization for the Advancement of Pure Research (Z.W.O.).

[1] T. P. Straatsma, H. J. C. Berendsen, and J. P. M. Postma, J. Chem. Phys. **85**, 6720 (1986).
[2] M. Born, Z. Phys. **1**, 45 (1920).
[3] J. D. Bernal and F. D. Fowler, J. Chem. Phys. **1**, 515 (1933).

[4] W. M. Latimer, K. S. Pitzer, and C. M. Slanksy, J. Chem. Phys. **7**, 108 (1939).

[5] R. M. Noyes, J. Am. Chem. Soc. **84**, 514 (1962).

[6] K. J. Laidler and J. S. Muirhead-Gould, Trans. Faraday Soc. **63**, 953 (1967).

[7] H. Block and S. M. Walker, Chem. Phys. Lett. **19**, 363 (1973).

[8] P. J. Stiles, Aust. J. Chem. **33**, 1389 (1980).

[9] D. L. Beveridge and G. W. Schnuelle, J. Phys. Chem. **78**, 2064 (1974).

[10] G. W. Schnuelle and D. L. Beveridge, J. Phys. Chem. **79**, 2566 (1975).

[11] J. G. Kirkwood, J. Chem. Phys. **2**, 351 (1934).

[12] D. L. Beveridge and G. W. Schnuelle, J. Phys. Chem. **79**, 2562 (1975).

[13] L. Onsager, J. Am. Chem. Soc. **58**, 1486 (1936).

[14] K. G. Spears and S. H. Kim, J. Phys. Chem. **80**, 673 (1976).

[15] K. G. Spears, J. Chem. Phys. **57**, 1850 (1972).

[16] K. G. Spears, J. Phys. Chem. **81**, 186 (1977).

[17] B. T. Gowda and S. W. Benson, J. Phys. Chem. **86**, 1544 (1982).

[18] B. T. Gowda and S. W. Benson, J. Comput. Chem. **4**, 283 (1983).

[19] M. R. Mruzik, F. F. Abraham, and D. E. Schreiber, J. Chem. Phys. **64**, 481 (1976).

[20] H. Kistenmacher, H. Popkie, and E. Clementi, J. Chem. Phys. **61**, 799 (1974).

[21] I. Džidić and P. Kebarle, J. Phys. Chem. **74**, 1466 (1970).

[22] M. Arshadi, R. Yamdagni, and P. Kebarle, J. Phys. Chem. **74**, 1475 (1970).

[23] P. Perez, W. K. Lee, and W. Prohofsky, J. Chem. Phys. **79**, 388 (1983).

[24] S. S. Sung and P. C. Jordan, J. Chem. Phys. **85**, 4045 (1986).

[25] P. Cieplak, T. P. Lybrand, and P. A. Kollman, J. Chem. Phys. **86**, 6393 (1987).

[26] M. Mezei and D. L. Beveridge, J. Chem. Phys. **74**, 622 (1981).

[27] M. Mezei and D. L. Beveridge, J. Chem. Phys. **74**, 6902 (1981).

[28] D. G. Bounds, Mol. Phys. **54**, 1335 (1985).

[29] G. I. Szász and K. Heinzinger, J. Chem. Phys. **79**, 3467 (1983).

[30] R. W. Impey, P. A. Madden, and I. R. McDonald, J. Phys. Chem. **87**, 5071 (1983).

[31] H. L. Nguyen and S. A. Adelman, J. Chem. Phys. **81**, 4564 (1984).

[32] M. A. Wilson, A. Pohorille, and L. R. Pratt, J. Chem. Phys. **83**, 5832 (1985).

[33] M. Berkowitz and W. Wan, J. Chem. Phys. **86**, 376 (1987).

[34] J. Chandrasekhar and W. L. Jorgensen, J. Chem. Phys. **77**, 5080 (1982).

[35] W. L. Jorgensen and J. Gao, J. Phys. Chem. **90**, 2174 (1986).

[36] E. Spohr and K. Heinzinger, J. Chem. Phys. **84**, 2304 (1986).

[37] M. Rao and B. J. Berne, J. Phys. Chem. **85**, 1498 (1981).

[38] P. H. Berens, D. H. J. Mackay, G. M. White, and K. R. Wilson, J. Chem. Phys. **79**, 2375 (1983).

[39] D. Frenkel and A. J. C. Ladd, J. Chem. Phys. **81**, 3188 (1984).

[40] H. J. C. Berendsen, J. P. M. Postma, and W. F. van Gunsteren, in *Molecular Dynamics and Protein Structure*, edited by J. Hermans (Polycrystal Book Service, Western Springs, Illinois, 1985), p. 43.

[41] T. P. Straatsma, Ph. D. thesis, University of Groningen, 1987.

[42] J. P. M. Postma, Ph. D. thesis, University of Groningen, 1985.

[43] A. Cross, Chem. Phys. Lett. **128**, 198 (1986).

[44] M. Mezei, J. Chem. Phys. **86**, 7084 (1987).

[45] J. P. M. Postma, H. J. C. Berendsen, and J. R. Haak, Faraday Symp. Chem. Soc. **17**, 55 (1982).

[46] S. Nosé, J. Chem. Phys. **81**, 511 (1984).

[47] S. Nosé, Mol. Phys. **52**, 255 (1984).

[48] A. Branka and M. Parrinello, Mol. Phys. **58**, 989 (1986).

[49] D. A. McQuarrie, in *Statistical Thermodynamics* (Harper and Row, New York, 1973).

[50] H. J. C. Berendsen, J. P. M. Postma, W. F. van Gunsteren, A. DiNola, and J. R. Haak, J. Chem. Phys. **81**, 3684 (1984).

[51] H. J. C. Berendsen and W. F. van Gunsteren, in *The Physics of Superionic Conductors and Electrode Materials*, NATO ASI Ser. B: Physics, Vol. 92, edited by J. W. Perram (Plenum, London, 1983), p. 221.

[52] J. P. Ryckaert, G. Ciccotti, and H. J. C. Berendsen, J. Comp. Phys. **23**, 327 (1977).

[53] W. F. van Gunsteren and H. J. C. Berendsen, Mol. Phys. **34**, 1311 (1977).

[54] H. J. C. Berendsen, J. P. M. Postma, W. F. van Gunsteren, and J. Hermans, *Intermolecular Forces*, edited by B. Pullman (Reidel, Dordrecht, 1981), p. 331.

[55] F. H. Stillinger and A. Rahman, J. Chem. Phys. **60**, 1545 (1974).

[56] F. H. Stillinger and C. W. David, J. Chem. Phys. **69**, 1473 (1978).

[57] G. D. Zeiss and W. J. Meath, Mol. Phys. **30**, 161 (1975).

[58] W. F. van Gunsteren, Mol. Phys. **40**, 1015 (1980).

[59] K. Remerie, Ph.D. thesis, University of Groningen, 1984.

[60] D. L. Beveridge, M. Mezei, P. K. Mehrotra, F. T. Marchese, G. Ravishanker, T. R. Vasu, and S. Swaminathan, Adv. Chem. **204**, 297 (1983).

[61] W. L. Jorgensen, J. Chandrasekhar, J. D. Madura, R. W. Impey, and M. L. Klein, J. Chem. Phys. **79**, 926 (1983).

[62] E. Clementi and H. Popkie, J. Chem. Phys. **57**, 1077 (1972).

[63] H. Kistenmacher, H. Popkie, and E. Clementi, J. Chem. Phys. **58**, 1689 (1973).

[64] H. Kistenmacher, H. Popkie, and E. Clementi, J. Chem. Phys. **58**, 5627 (1973).

[65] H. Kistenmacher, H. Popkie, and E. Clementi, J. Chem. Phys. **59**, 5842 (1973).

[66] P. D. Dacre, Mol. Phys. **51**, 633 (1984).

[67] D. G. Bounds and P. J. Bounds, Mol. Phys. **50**, 1125 (1983).

[68] D. G. Bounds and P. J. Bounds, Mol. Phys. **50**, 25 (1983).

[69] I. Ortega Blake, J. C. Barthelat, E. Costes-Puech, E. Oliveros, and J. P. Daudey, J. Chem. Phys. **76**, 4130 (1982).

[70] G. H. F. Diercksen and W. P. Kraemer, Chem. Phys. Lett. **5**, 570 (1970).

[71] P. A. Kollman and I. D. Kuntz, J. Am. Chem. Soc. **94**, 9236 (1972).

[72] P. A. Kollman and I. D. Kuntz, J. Am. Chem. Soc. **96**, 4766 (1974).

[73] W. F. van Gunsteren, *GROMOS Reference Manual*, BIOMOS B. V. (Nijenborgh 16, Groningen, The Netherlands, 1987).

[74] O. Teleman and P. Ahlstrom, J. Am. Chem. Soc. **108**, 4333 (1986).

[75] O. Teleman, Ph.D. thesis, University of Lund, 1986.

[76] J. M. Caillol, D. Levesque, and J. J. Weis, J. Chem. Phys. **85**, 6645 (1986).

[77] O. Matsuoka, E. Clementi, and M. Yoshimine, J. Chem. Phys. **64**, 1351 (1976).

[78] J. Chandrasekhar, D. C. Spellmeyer, and W. L. Jorgensen, J. Am. Chem. Soc. **106**, 903 (1984).

[79] H. L. Friedman and C. V. Krishnan, in *Water a Comprehensive Treatise*, edited by F. Franks (Plenum, New York, 1973).

[80] T. P. Lybrand, I. Ghosh, and J. A. McCammon, J. Am. Chem. Soc. **107**, 7793 (1985).

[81] C. L. Brooks, J. Phys. Chem. **90**, 6680 (1986).